ChemPubSoc Europe

DOI: 10.1002/cphc.201700607

CHEMPHYSCHEM Communications

Beyond the Hammett Effect: Using Strain to Alter the Landscape of Electrochemical Potentials

Matthew D. Casselman,[a] Corrine F. Elliott,[a] Subrahmanyam Modekrutti,[a] Peter L. Zhang,[a] Sean R. Parkin,[a] Chad Risko,*[a, b] and Susan A. Odom*[a]

We dedicate this manuscript to Professor John E. Anthony in honor of his 50th birthday.

The substitution of sterically bulky groups at precise locations along the periphery of fused-ring aromatic systems is demonstrated to increase electrochemical oxidation potentials by preventing relaxation events in the oxidized state. Phenothiazines, which undergo significant geometric relaxation upon oxidation, are used as fused-ring models to showcase that electron-donating methyl groups, which would generally be expected to lower oxidation potential, can lead to increased oxidation potentials when used as the steric drivers. Reduction events remain inaccessible through this molecular design route, a critical characteristic for electrochemical systems where high oxidation potentials are required and in which reductive decomposition must be prevented, as in high-voltage lithium-ion batteries. This study reveals a new avenue to alter the redox characteristics of fused-ring systems that find wide use as electroactive elements across a number of developing technologies.

The electrochemical redox potentials of π-conjugated organic molecules and polymers influence a material's performance in applications such as organic electronics, energy collection, energy storage, and catalysis, to name but a few. In these systems, the general prescriptions to control redox potentials involve substitution with electron-donating and/or electron-withdrawing groups, making use of the well-known Hammett constants as predictors of the extent of the change in redox potentials,[1] and/or modifying the length of the π-conjugation pathway, as in the transition from ethylene to butadiene to hexatriene and beyond. Another route to modify molecular redox potentials exploits strain-induced disruptions of the π-conjugated framework.[2] Such chemical modifications typically use so-called "bulky" substituents to manipulate dihedral torsions among the π-conjugated moieties that make up the molecular systems. Prime examples include biphenyl (or more generally oligo- or polyphenylenes), in which substituents incorporated at the 2, 2′, 6, and/or 6′ positions increase the twist angle between the phenyl groups, and oligothiophenes, where similar tactics are employed with substituents placed at the 3 and/or 4 positions.[3] Notably, these considerations have been widely used in the development of π-conjugated polymers for electronics and solar cell applications. Strain has also been used to impose curvature on π-conjugated networks to alter optical and/or redox characteristics, for example, in fullerenes,[4] cyclized stilbenes,[5] and twisted acenes (so-called "twistacenes").[6] In each of these latter systems, the π-conjugated networks are strained in both the ground (neutral) and ionized (oxidized or reduced) electronic states. Taking these studies as inspiration, we demonstrate molecular design principles to dictate the relaxation processes of π-conjugated molecules through strain solely in their ionized state, while imparting minimal change to the ground-state characteristics, as an effective way to synthetically control redox potentials.

Our interest in this idea stemmed from the study of a series of phenothiazine derivatives, in which the geometry of the oxidized (radical-cation) state tends to be planar, while the neutral ground state is bent.[7] In particular, for *N*-substituted phenothiazines (Figure 1, left), we observed a correlation between

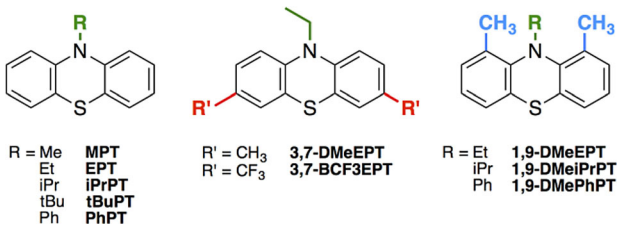

Figure 1. Representation of the structures of various phenothiazine derivatives.

the degree of molecular bending (referred to as the "butterfly angle") of the radical-cation geometry and the ease of oxidation: From ethyl to *iso*-propyl to *tert*-butyl (EtPT, *i*PrPT, *t*BuPT), the increased substituent size led to a larger radical-cation butterfly angle and higher-potential oxidation events (Table 1). Importantly, this effect is opposite to what one would predict based on the Hammett constants of the substituents, suggesting that preventing planarization in radical cations may raise oxidation potentials, regardless of the substituent's Hammett constant.

The possibility of raising phenothiazine oxidation potentials without incorporating electron-withdrawing groups intrigued

[a] Dr. M. D. Casselman, C. F. Elliott, Dr. S. Modekrutti, P. L. Zhang, Dr. S. R. Parkin, Prof. Dr. C. Risko, Prof. Dr. S. A. Odom
Department of Chemistry, University of Kentucky
Lexington, KY, 40506 (USA)
E-mail: susan.odom@uky.edu
chad.risko@uky.edu

[b] Prof. Dr. C. Risko
Center for Applied Energy Research
University of Kentucky, Lexington, KY, 40511 (USA)

Supporting Information and the ORCID identification number(s) for the author(s) of this article can be found under https://doi.org/10.1002/cphc.201700607.

Table 1. Adiabatic ionization potentials (IP), half-wave first oxidation potentials ($E_{1/2}^{+/0}$) versus $Cp_2Fe^{+/0}$, and neutral and radical cation butterfly angles.

Compound	IP [eV][a]	$E_{1/2}^{+/0}$ [V] [b]	Butterfly angles [°][a]	
			Neutral	Radical Cation
MPT	6.58	0.31[e]	143.4 (143.7)[d]	165.2 (177.8)
EPT	6.48	0.27	138.7 (136.8)[d]	171.4 (173.8)
iPrPT	6.52	0.33[e]	142.6 (137.9)[e]	160.7
tBuPT	6.67	0.53[e]	134.2 (135.0)[e]	148.3
PhPT	6.34	0.26[e]	149.5 (162.3)[e]	180.0
3,7-DMeEPT	6.24	0.13[f]	138.8 (149.3)[f]	171.1
3,7-BCF3EPT	7.06	0.61[f]	139.7 (144.5–152.1)[g]	171.1 (164.5)[g]
1,9-DMeEPT	6.68	0.55	143.1 (146.5)	156.6
1,9-BCF3EPT	7.21	–	141.8	159.0
1,9-DMeiPrPT	6.76	0.68	132.5 (134.1)	147.5
1,9-DMePhPT	6.85	0.86[c]	132.4 (134.9)	137.2

[a] DFT calculations at the B3LYP/6-311G(d,p) level of theory; X-ray crystallographic values in parentheses. [b] CV performed with 1.6 mM in 0.1 M nBu_4NPF_6/DCM at 100 mV s^{-1}. [c] Oxidation was irreversible. [d] Ref. [11]. [e] Ref. [7b]. [f] Ref. [9d]. [g] Multiple molecules in asymmetric unit, Ref. [12].

us due to our work in overcharge protection of lithium-ion batteries (LIBs). Maximizing both the energy density and the durability of a LIB requires charging to a precise voltage: Below that potential, the full capacity of the cell is not utilizied; at higher potentials, a cell enters overcharge, a condition that can seriously degrade LIBs and lead to hazardous operating conditions.[8] Molecular redox shuttles can be used to mitigate excess current in overcharging batteries by spatially ferrying charge via a series of electron-transfer reactions, oxidizing to their radical-cation form at the cathode and reducing to their neutral form at the anode. For molecules designed to mitigate overcharge in LIBs, chemical substitutions are made to adjust the oxidation potentials with respect to the reduction potential of the cathode to ensure that the shuttles become redox active just after a cell is fully charged.[8] Extensive overcharge protection has been demonstated for lower-voltage $LiFePO_4$ cathodes,[8a,9] which requires shuttles that oxidize at potentials of 3.8 to 3.9 V vs. $Li^{+/0}$. However, the protection of higher-voltage cathodes (e.g. $LiCoO_2$, $LiMnO_2$, and $LiNi_{1/3}Mn_{1/3}Co_{1/3}O_2$) require oxidation potentials of 4.2 V or higher, and no shuttle has provided extensive protection in cells containing graphitic anodes.

The road to shuttles with higher oxidation potential via the incorporation of strong electron-withdrawing groups on viable low-voltage shuttles can introduce perils to the framework of LIBs. Electron-withdrawing substituents shift both the oxidation *and* reduction potentials to more-positive values, producing compounds that are more susceptible to decomposition via reactions that take place following reduction to the radical anion at the anode.[7a,10] Premature failure of phenothiazine redox shuttles containing chlorine, bromine, cyano, or nitro groups can be traced back to their having reduction potentials >0 V vs. $Li^{+/0}$.[7a,10e] Dimethoxybenzene derivatives containing strongly electron-withdrawing groups exhibit short-lived overcharge protection when incorporated into lithium-ion cells containing graphite anodes,[10a–d] perhaps as a result of reductive decomposition at the anode/electrolyte interface. This hypothesis is supported by reports of the redox shuttle 1,4-di-*tert*-butyl-2,5-bis(2,2,2-trifluoroethoxy)benzene surviving 2× longer in cells containing the $Li_4Ti_5O_{12}$ anode when compared to LIBs with either the highly reducing graphitic or lithium-metal anodes.[10b] As such, the incorporation of strongly electron-withdrawing groups is a problematic route for molecules that require stability at both high and low redox potentials. Thus, a new approach for designing stable, high-voltage redox shuttles is needed.

Inspired by studies of molecular strain, we sought to address whether the strategic placement of substituents on the phenothiazine core could be used to tune molecular redox characteristics through geometric constraints, with minimal impact by the substituent electronic effects. Our hypothesis was the following: Deliberate incorporation of substituents around the periphery of the phenothiazine core would disrupt the relaxation of the radical-cation state, thereby increasing the oxidation potential compared to the unsubstituted system. This hypothesis led us to evaluate derivatives of *N*-substituted phenothiazines where substituents were incorporated at positions *ortho* to the nitrogen atom (1 and 9 positions), which we envisioned would prevent planarization of the oxidized species through steric interactions with the *N*-alkyl group. We compared the electrochemical characteristics of these derivatives to a parent compound with only an *N* substituent, and to derivatives in which the same substituents are incorporated at positions *para* to the nitrogen atom (3 and 7 positions) so that planarization in the oxidized state remains possible and the full electronic effects of the substituents are play. For the sake of clarity, we will focus our discussion on the *N*-ethyl derivatives, where EPT is the parent; 1,9-DMeEPT the crowded derivative; and 3,7-DMeEPT the uncrowded analogue (Figure 1).

At the outset of the investigation, we made use of density functional theory (DFT) calculations at the B3LYP/6-311G(d,p) level to predict molecular geometries in the neutral and radical-cation states, as well as the adiabatic and vertical ionization potentials (IPs), of various substituted phenothiazines. The neutral geometries of EPT, 3,7-DMeEPT, and 1,9-DMeEPT are quite similar, with the butterfly angles showing little variation (139–143°). However, as radical cations, EPT and 3,7-DMeEPT are significantly more planar (171°) than 1,9-DMeEPT (157°) (Table 1); note that 180° represents a fully planar phenothiazine. Similar trends are noted for the other 3,7- and 1,9-substituted phenothiazines in the series.

DFT calculations predict 3,7-DMeEPT to have an adiabatic IP 0.24 eV smaller than EPT, consistent with measured oxidation potentials[9c] and expectations based on the electron-donating capability of a methyl group. However, 1,9-DMeEPT has an IP 0.20 eV larger than EPT (Table 1). Thus, for the two DMeEPT constitutional isomers, we observe a difference in IP of 0.44 eV. The IP trends are similar for 3,7-BCF3EPT and 1,9-BCF3EPT, with

1,9-BCF3EPT having a larger IP, though the IP range is smaller (0.15 V). These results showcase the considerable impact that steric crowding of the radical-cation state can have on increasing the IP.

Similar trends are observed for the vertical IPs (Table S1). Notably, the relaxation energy (λ) in the radical-cation potential energy surface is smaller for 1,9-DMeEPT (at 0.27 eV) than for EPT and 3,7-DMeEPT (both at 0.40 eV), signifying the impact of the methyl groups at the 1 and 9 positions in limiting radical cation relaxation to a more planar configuration. Moreover, the vertical IPs for EPT and 1,9-DMeEPT are quite similar (differing by 0.07 eV), while that of 3,7-DMeEPT is much smaller than EPT (by 0.23 eV), revealing the differences in the electronic impact of methyl substituents in the 1 and 9 vs. 3 and 7 positions. Potential energy surfaces displaying these differences in terms of the adiabatic and vertical IPs and relaxation energies are represented in Figure 2.

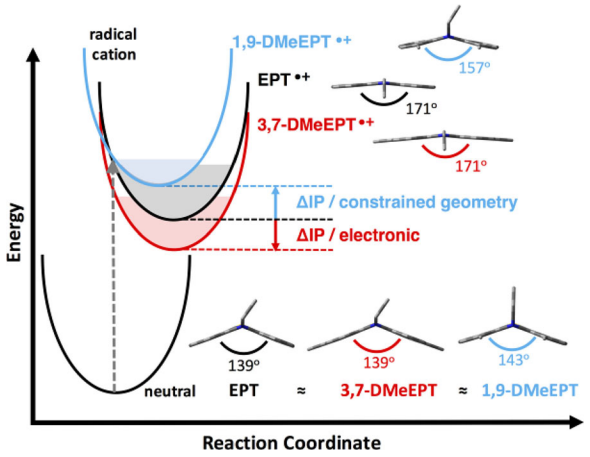

Figure 2. Representations of the potential energy surfaces for the oxidation of EPT, 3,7-DMeEPT, and 1,9-DMeEPT. The gray arrow with a dotted line depicts the vertical ionization process from ground-state, neutral species. Shaded regions represent relaxation energies in the radical-cation potential energy surfaces. The change in IP is given by ΔIP.

With computational results in hand that supported our hypothesis, we prepared 1,9-DMeEPT and related *N-iso*-propyl (1,9-DMe*i*PrPT) and *N*-phenyl (1,9-DMePhPT) derivatives, as shown in Scheme 1. Bis(*o*-tolyl)amine was synthesized from *o*-bromotoluene in a palladium-catalyzed amination with urea. Elemental sulfur was used to form the phenothiazine ring. Deprotonation of the amine followed by treatment with bromoethane or 2-bromopropane yielded 1,9-DMeEPT or 1,9-DMe*i*PrPT, respectively. A palladium-catalyzed reaction with bromobenzene yielded 1,9-DMePhPT.

Solid-state butterfly angles show good agreement with DFT calculations (Table 1). Importantly, the trends in oxidation potentials from CV experiments (Figure 3, polarographic conventions) validated our hypothesis and computational results. Unlike 3,7-DMeEPT, which is more easily oxidized than EPT (by 0.14 V), 1,9-DMeEPT is harder to oxidize than EPT (by 0.28 V). Moreover, as the size of the radical-cation butterfly angle increases within the series of 1,9-dimethyl-substituted phenothiazines, the oxidation potentials further increase. Of the three 1,9-dimethyl-substituted derivatives, 1,9-DMePhPT has the highest oxidation potential. Notably, this trend does not follow that of the solely *N*-substituted equivalents (*i*PrPT is harder to oxidize than both EPT and PhPT),[7b] though within each series of three compounds, the oxidation potentials follow the same trends as the calculated adiabatic IPs and radical-cation butterfly angles. Furthermore, scans of the full electrochemical window (Figure S6) show that reduction events remain inaccessible throughout the series, with solvent reduction occurring before a reduction event could be observed.

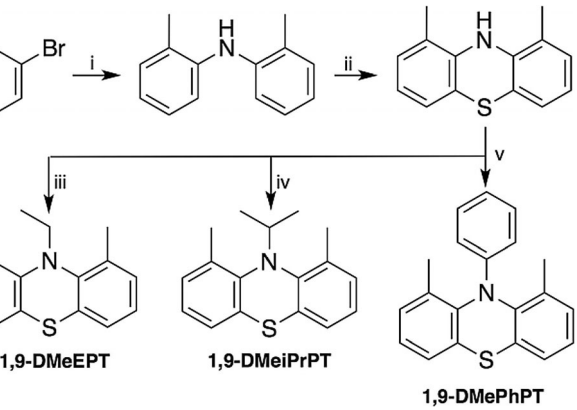

Scheme 1. Synthesis of 1,9-DMeEPT, 1,9-DM*i*PrPT, and 1,9-DMePhPT: i) urea, $Pd(dba)_2$, $tBu_3{\cdot}HBF_4$, NaO*t*Bu, dioxane, reflux, o/n, ii) S, cat. I_2, ODCB, 180 °C, 8 h, iii) 1. NaH, DMF, THF, rt, 10 min, 2. EtBr, 60 °C, o/n, iv) 1. NaH, DMF, THF, 0 °C, 5 min, 2. *i*PrBr, rt, o/n, v) PhBr, $Pd(dba)_2$, $tBu_3{\cdot}HBF_4$, NaO*t*Bu, PhMe, reflux, o/n.

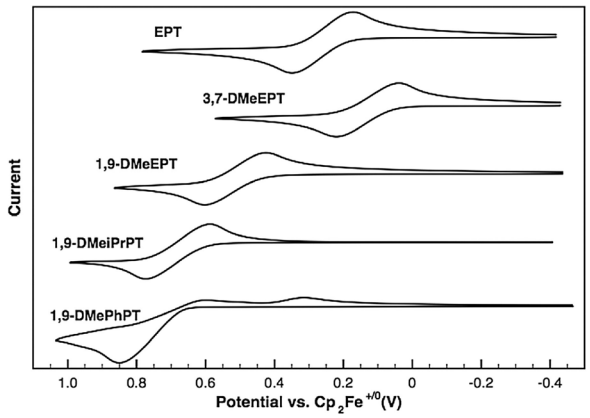

Figure 3. Cyclic voltammograms of EPT, 3,7-DMeEPT, 1,9-DMeEPT, 1,9-DM*i*PrPT, and 1,9-DMePhPT at 1.6 mM in 0.1 M nBu_4NPF_6 in DCM. Voltammograms are calibrated to $Cp_2Fe^{+/0}$ at 0 V, and recorded at 100 mV s^{-1}.

UV/Vis absorption spectroscopy was used to explore electronic transitions in the neutral and radical-cation states. While the absorption profiles of neutral EPT and 3,7-DMeEPT are nearly identical, the absorption onsets of the 1,9-dimethyl-substituted derivatives are slightly blue-shifted (Figure 4a). These changes in energy, although small, are consistent with trends in the energy of the $S_0 \rightarrow S_1$ transition determined by time-dependent DFT (TD-DFT) calculations (Table S1). UV/Vis spectra of the radical cations, generated by chemical oxidation, further

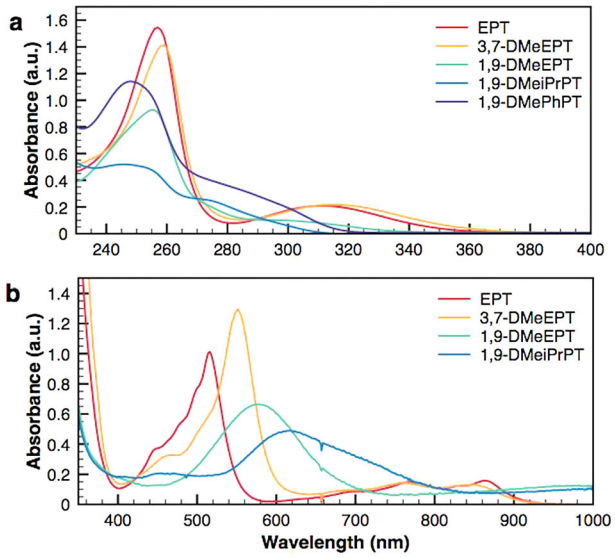

Figure 4. UV/Vis absorption spectra of EPT, 3,7-DMeEPT, 1,9-DMeEPT, 1,9-DMe*i*PrPT, and 1,9-DMePhPT in their neutral (a) and radical cation (b) forms at 14 μM and 0.1 mM, respectively, in DCM. Note: No spectrum is reported for the 1,9-DMePhPT radical cation due to its irreversible first oxidation event.

reflect differences in the oxidized species (Figure 4b). The absorption spectra of the radical cations of EPT and 3,7-DMeEPT show profiles consistent with the radical cations of several phenothiazine derivatives prepared in our laboratory: intense absorption features between 500–600 nm and low-energy, low-intensity bands between 650–950 nm.[7b,13] By contrast, the analogous absorption features for the 1,9-disubstituted derivatives occur at lower energies. These trends in transition energies are confirmed by TD-DFT calculations (Table S1). Our results suggest that variation in placement of methyl groups affects the electronic gap between the HOMO-1 and HOMO (using the nomenclature of the neutral species), which in turn influences the $D_1 \rightarrow D_2$ transition of the radical cation that is predominately HOMO-1→SOMO (singly-occupied molecular orbital) in nature. From DFT calculations, the HOMO of EPT and 1,9-DMeEPT are nearly isoenergetic, while that of 3,7-DMeEPT is energetically destabilized; this observation is consistent with the trends of the computed vertical IPs, confirming the validity of a Koopmans' theorem[14] (Janak's theorem[15] in the context of DFT) estimate of the vertical IPs based on the HOMO energies. However, the HOMO-1 of 3,7-DMeEPT and 1,9-DMeEPT are of similar energy and energetically destabilized when compared to EPT, revealing the comparable electronic impact of the methyl groups on the HOMO-1 regardless of the methyl group's location on the phenothiazine. The combination of these effects results in a smaller HOMO-1 to HOMO energy gap for 1,9-DMeEPT, which is found here to translate to a smaller first-excited-state transition energy of the radical cation.

In summary, by positioning traditionally electron-donating substituents in close proximity to the *N* substituent, we disrupted the relaxation of the phenothiazine radical cation state and increased the oxidation potentials relative to their counterparts that are able to fully relax. This approach offers a strain-induced modulation of electrochemical properties orthogonal to conventional tuning by substituent character. By disrupting relaxation pathways in fused-ring systems, we hope to identify new organic materials with higher oxidation potentials while limiting access to reduction events.

Acknowledgements

This work was funded by the National Science Foundation's Division of Chemistry (Award 1300653) and EPSCoR Program (Award 1355438). CFE thanks the Division of Organic Chemistry of the American Chemical Society for a Summer Undergraduate Research Fellowship. SAO and CR thank the University of Kentucky for start-up funding.

Conflict of interest

The authors declare no conflict of interest.

Keywords: conjugation · electronic structure · redox chemistry · strained molecules · substituent effects

[1] a) L. P. Hammett, *J. Am. Chem. Soc.* **1937**, *59*, 96–103; b) M. J. S. Dewar, P. J. Grisdale, *J. Am. Chem. Soc.* **1962**, *84*, 3539–3541; c) M. J. S. Dewar, P. J. Grisdale, *J. Am. Chem. Soc.* **1962**, *84*, 3548–3553; d) C. Hansch, A. Leo, R. W. Taft, *Chem. Rev.* **1991**, *91*, 165–195; e) K. Bowden, E. J. Grubbs, in *Progress in Physical Organic Chemistry*, Wiley, Hoboken, **2007**, pp. 183–224.

[2] a) J. H. D. Eland, *Int. J. Mass Spectrom. Ion Phys.* **1969**, *2*, 471–484; b) J. P. Maier, D. W. Turner, *Faraday Discuss. Chem. Soc.* **1972**, *54*, 149–167; c) L. Andrews, R. T. Arlinghaus, C. K. Payne, *J. Chem. Soc. Faraday Trans. 2* **1983**, *79*, 885–895; d) J. Cioslowski, S. T. Mixon, *J. Am. Chem. Soc.* **1992**, *114*, 4382–4387; e) M. Rubio, M. Merchán, E. Ortí, *Theor. Chim. Acta* **1995**, *91*, 17–29; f) A. Karpfen, C. H. Choi, M. Kertesz, *J. Phys. Chem. A* **1997**, *101*, 7426–7433; g) S. Tsuzuki, T. Uchimaru, K. Matsumura, M. Mikami, K. Tanabe, *J. Chem. Phys.* **1999**, *110*, 2858–2861; h) J. C. Sancho-García, A. J. Pérez-Jiménez, *J. Phys. B* **2002**, *35*, 1509; i) D. Vonlanthen, A. Rudnev, A. Mishchenko, A. Käslin, J. Rotzler, M. Neuburger, T. Wandlowski, M. Mayor, *Chem. Eur. J.* **2011**, *17*, 7236–7250.

[3] a) G. R. Hutchison, M. A. Ratner, T. J. Marks, *J. Am. Chem. Soc.* **2005**, *127*, 2339–2350; b) S. S. Zade, M. Bendikov, *Chem. Eur. J.* **2007**, *13*, 3688–3700.

[4] R. C. Haddon, *Science* **1993**, *261*, 1545–1550.

[5] Q. Chen, M. T. Trinh, D. W. Paley, M. B. Preefer, H. Zhu, B. S. Fowler, X. Y. Zhu, M. L. Steigerwald, C. Nuckolls, *J. Am. Chem. Soc.* **2015**, *137*, 12282–12288.

[6] a) J. D. Debad, S. K. Lee, X. Qiao, J. R. A. Pascal, A. J. Bard, *Acta. Chem. Scand.* **1998**, *52*, 45–50; b) H. M. Duong, M. Bendikov, D. Steiger, Q. Zhang, G. Sonmez, J. Yamada, F. Wudl, *Org. Lett.* **2003**, *5*, 4433–4436; c) J. Xiao, Y. Divayana, Q. Zhang, H. M. Doung, H. Zhang, F. Boey, X. W. Sun, F. Wudl, *J. Mater. Chem.* **2010**, *20*, 8167–8170.

[7] a) M. D. Casselman, A. P. Kaur, K. A. Narayana, C. F. Elliott, C. Risko, S. A. Odom, *Phys. Chem. Chem. Phys.* **2015**, *17*, 6905–6912; b) K. A. Narayana, M. D. Casselman, C. F. Elliott, S. Ergun, S. R. Parkin, C. Risko, S. A. Odom, *ChemPhysChem* **2015**, *16*, 1179–1189.

[8] a) J. Chen, C. Buhrmester, J. R. Dahn, *Electrochem. Solid-State Lett.* **2005**, *8*, A59–A62; b) Z. Chen, Y. Qin, K. Amine, *Electrochim. Acta* **2009**, *54*, 5605–5613.

[9] a) J. R. Dahn, J. Jiang, L. M. Moshurchak, M. D. Fleischauer, C. Buhrmester, L. J. Krause, *J. Electrochem. Soc.* **2005**, *152*, A1283–A1289; b) L. M. Moshurchak, C. Buhrmester, R. L. Wang, J. R. Dahn, *Electrochim. Acta* **2007**, *52*, 3779–3784; c) S. Ergun, C. F. Elliott, A. P. Kaur, S. R. Parkin, S. A. Odom, *Chem. Commun.* **2014**, *50*, 5339–5341; d) A. P. Kaur, S. Ergun, C. F. Elliott, S. A. Odom, *J. Mater. Chem. A* **2014**, *2*, 18190–18193;

e) A. P. Kaur, C. F. Elliott, S. Ergun, S. A. Odom, *J. Electrochem. Soc.* **2016**, *163*, A1 – A7.

[10] a) Z. Chen, K. Amine, *Electrochem. Commun.* **2007**, *9*, 703 – 707; b) L. M. Moshurchak, W. M. Lamanna, M. Bulinski, R. L. Wang, R. R. Garsuch, J. Jiang, D. Magnuson, M. Triemert, J. R. Dahn, *J. Electrochem. Soc.* **2009**, *156*, A309 – A312; c) L. Zhang, Z. Zhang, H. Wu, K. Amine, *Energy Environ. Sci.* **2011**, *4*, 2858 – 2862; d) J. Huang, N. Azimi, L. Cheng, I. A. Shkrob, Z. Xue, J. Zhang, N. L. Dietz Rago, L. A. Curtiss, K. Amine, Z. Zhang, L. Zhang, *J. Mater. Chem. A* **2015**, *3*, 10710 – 10714; e) A. P. Kaur, M. D. Casselman, C. F. Elliott, S. R. Parkin, C. Risko, S. A. Odom, *J. Mater. Chem. A* **2016**, *4*, 5410 – 5414.

[11] S. S. C. Chu, D. Van der Helm, *Acta Crystallogr. Sect. B* **1974**, *30*, 2489 – 2490.

[12] S. Ergun, M. D. Casselman, A. P. Kaur, S. R. Parkin, S. A. Odom, unpublished results.

[13] S. Ergun, C. F. Elliott, A. P. Kaur, S. R. Parkin, S. A. Odom, *J. Phys. Chem. C* **2014**, *118*, 14824 – 14832.

[14] T. Koopmans, *Physica* **1934**, *1*, 104 – 113.

[15] J. F. Janak, *Phys. Rev. B* **1978**, *18*, 7165 – 7168.

Manuscript received: June 6, 2017
Accepted manuscript online: June 7, 2017
Version of record online: ■■ ■■, 0000

COMMUNICATIONS

M. D. Casselman, C. F. Elliott, S. Modekrutti, P. L. Zhang, S. R. Parkin, C. Risko, S. A. Odom**

■■ – ■■

Beyond the Hammett Effect: Using Strain to Alter the Landscape of Electrochemical Potentials

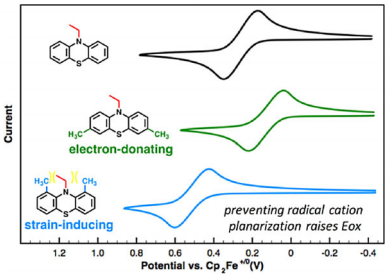

Through the strategic placement of otherwise electron-donating methyl groups at the positions *ortho* to nitrogen, planarization of the phenothiazine radical cation is prevented, thus raising the oxidation potential of this compound (blue) compared to its *para*-substituted isomer (green) and parent compound (black).